



# Enthalpies of mixing for alloys liquid below room temperature determined by oxidative solution calorimetry

Michael Bustamante<sup>1</sup> · Kristina Lilova<sup>2</sup> · Alexandra Navrotsky<sup>1,2</sup>  · Jean-Philippe Harvey<sup>3</sup> · Kentaro Oishi<sup>3</sup>

Received: 3 August 2023 / Accepted: 1 March 2024 / Published online: 13 May 2024  
© Akadémiai Kiadó, Budapest, Hungary 2024

## Abstract

Fusible alloys, in particular gallium-based alloys liquid below room temperature (Ga-LMA), have applications in soft robotics, microelectronics, self-healing battery components, and 2D materials synthesis, making the study of their thermodynamic properties critical for the improvement and development of hybrid materials. To determine the enthalpies of formation/mixing of the eutectics for the binary Ga–In, the ternary Ga–In–Sn, and the quaternary Ga–In–Sn–Zn systems, a novel experimental calorimetric technique based on oxidative solution calorimetry was developed. The experimental results for the binary eutectic are consistent with previous data obtained by direct reaction and solution calorimetry, demonstrating the viability and precision of the experimental technique presented, which can now be extended to a large variety of liquid alloy systems at or below room temperature. To our knowledge, the heats of mixing in the ternary and quaternary systems represent the first reported experimental values. Both standard geometrical models and FactSage were used to calculate the enthalpies of mixing for these alloys, which agreed with the experimental data, providing a foundation to analyze the thermodynamics of other unknown Ga-based alloys.

**Keywords** Gallium alloys · Alloys liquid below room temperature · Experimental thermodynamics · Oxidative solution calorimetry · Enthalpy models

## Introduction

Gallium-based liquid metal alloys (Ga-LMA) are integral to soft robotics, microelectronics, self-healing battery components, and 2D materials synthesis [1–4]. They have useful properties such as low toxicity and low vapor pressure relative to mercury (Hg), and exhibit good material stability/compatibility [5] with potentially tunable room temperature phase transitions and intermetallics formation [1, 2, 6].

These alloys also have high volumetric enthalpy of fusion and thermal conductivity in addition to much faster heat absorption/dissipation rates in comparison with other phase change materials (PCMs) [7–9]. Potentially widening the application of these alloys into microprocessor technology, provided that the natural corrosion and supercooling effects are mitigated or harnessed effectively [10]. This broad applicability justifies the current interest for Ga-LMA and the steady increase of available experimental data [11]. Nonetheless, there are still many systems and material properties for Ga and its eutectics with indium (In), and tin (Sn) that have not been fully explored. These include detailed corrosion/oxidation mechanisms when the Ga present in these alloys dissolves or comes in contact with other metal/metalloid substrates [10, 12], a major interest for cooling and additive manufacturing of electronics [13]. Other areas that lack experimental information include Ga-LMA with added solid particles (which can be pure metals, oxides, and intermetallics) when synthesized or exposed to extreme pressures and temperatures. Most studies focus on functional composites produced at more reasonable manufacturing conditions [14–16]. The current data also extends to heat capacity

✉ Alexandra Navrotsky  
anavrotsky@asu.edu

<sup>1</sup> Ira A. Fulton School for Engineering of Matter, Transport, and Energy, Arizona State University, Tempe, AZ 85287, USA

<sup>2</sup> School of Molecular Sciences and Center for Materials of the Universe, Arizona State University, Tempe, AZ 85287, USA

<sup>3</sup> Center for Research in Computational Thermochemistry (CRCT), Department of Chemical Engineering, Polytechnique Montréal, Downtown Station Québec, P.O. Box 6079, Montréal, QC H3C 3A7, Canada

measurements and structural evolution studies of Ga, Ga–In, and Ga–In–Sn systems at a narrow set of experimental parameters [17–19]. High temperature thermodynamic studies in comparison include many binary, ternary, and more complex Ga alloys [20–23]. Of these, only a small subset focused on the thermodynamics of solid alloys of Ga, In, and Sn using various thermal analysis techniques [24–26].

Direct reaction calorimetry is an in-situ process in which metallic powders are mixed in an inert atmosphere with the appropriate stoichiometric ratios, pressed together, and dropped into a calorimeter at a temperature where they react to form alloys and compounds. The success of this methodology depends on the rapid and complete reaction of the powders without the formation of unwanted oxidation and/or side products. This technique has produced substantial data over the years [27, 28] and has been in use at several labs around the world [29–34]. However, the technique has not always been successful at producing reliable data, especially for some multicomponent alloys, due to the alloying characteristics (at the reaction temperature and upon cooling) of each of the components in the amalgam and how these affect the structural/compositional complexity of the sample mixture, making it more difficult to characterize through calorimetry [35].

Solution calorimetry in molten Sn at moderate temperatures (< 500 °C) [36] and in other alloys at higher temperatures (Ga, In, Al, etc.) [37, 38] has been effective for some systems, but, similarly to direct reaction calorimetry, it lacks general applicability due to its dependence on rapid component dissolution in the metallic solvent, restricted by the high melting points of metals, limited solubility of constituents in the metallic solvent, and again the increasing complexity of the final alloy/solvent solution as components increase. Furthermore, many alloys have oxygen (O<sub>2</sub>) sensitivity that cannot always be avoided at a wide range of temperatures, requiring rigorous O<sub>2</sub> control and careful sample handling. [36–38]

Consequently, a calorimetric method was developed and applied to a broader variety of alloys and compositions while eliminating the need for O<sub>2</sub> control over the sample at high temperature for long periods of time. This has led us to apply oxidative solution calorimetry in a molten oxide solvent, a technique that has been effective at enthalpy determinations for multicomponent alloys as well as chalcogenides by employing oxidizing conditions [39–41]. This technique is based on “drop solution” calorimetry, a process in which a sample is dropped from room temperature into a molten oxide solvent at 700–800 °C, causing rapid sample oxidation and dissolution upon contact with solvent. This process yields completely dissolved samples that can be represented through Hess’s law as oxides in solution in the salt solvent and, when appropriate, evolved gaseous species [42]. This technique employs low concentrations of the dissolved

products approaching infinite dilution in the molten oxide solvent, making the heats of solution obtained independent of the concentrations of dissolved species present, with minimal interaction effects of the dissolved cations in the melt, and no precipitation of interoxidic compounds during experiments [43]. Gas flow over and through the solvent enables atmosphere control, efficient transport of gas out of the calorimeter, and provides stirring for the melt. This procedure has been used extensively to determine enthalpies of formation and mixing in various multicomponent oxide systems [44, 45] as well as in some sulfides, selenides, and alloys [35, 46, 47]. This technique can be considered general as long as the final calorimetric products are fully dissolved in the molten salt solvent and have reproducible final states that can be represented accurately in thermodynamic cycles [43]. In our lab, to measure full dissolution and oxidation of metallic samples, a visual test prior to calorimetry via melting of the oxide solvent in a clear quartz crucible and subsequent drops of samples from room temperature into this open crucible containing solvent are made [48].

Oxidative solution calorimetry eliminates most of the constraints mentioned above for both the direct reaction and solution methods. Nevertheless, in its present form it cannot readily analyze alloys that are molten below or at room temperature, due to small glassware geometry and no direct liquid sample transport method to the reaction crucible. The goal of the present study is to modify this technique to be applicable to alloys molten at or below room temperature among other liquid materials stable at higher temperature.

Experimental data for enthalpies of formation and mixing for binary and ternary metallic systems form the input and underpinning for the determination of higher order alloy phase diagrams via the CALPHAD method. In this computational thermochemistry framework, optimized binary excess interactions for a given solution are interpolated using geometrical models into higher order systems. The main challenges when describing the energetic behavior of solid and liquid solutions are (1) how to account for nonideality in the configurational entropy of mixing contribution (including the potential presence of short/long range ordering) and (2) how to interpolate binary excess parameters into higher-order systems, especially near room temperature [49].

Geometrical models which are required to evaluate the enthalpy contribution of binary sub-systems into higher-order solutions are split into two types, symmetric which include those of Kohler and Maggiani among others [50–52] and asymmetric which include those of Toop, Hillert [50], Ouyang [53], and Chou [54, 55]. It should be noted however, there are no definitive rules to apply these geometrical models to higher order systems, so they have to be tested against available experimental data to discern the optimal model to be used in a specific system(s) [56]. These have been employed for comparisons with existing

ternary and quaternary experimental data, producing reasonable agreements favoring asymmetric energetic estimations [53–55, 57]. FactSage and other well established commercial CALPHAD-type calculation programs [58–61], allow the interchangeable use of these geometrical models to describe the energetics of multicomponent solutions. Such thermodynamic packages could work most effectively for complex Ga-based liquid alloys by providing user-friendly interfaces, extensive databases of optimized enthalpy of mixing for many of their binary alloy solutions and compounds to produce reasonably accurate thermodynamic properties for multicomponent systems. Integration of new experimental data along with further updates to the computation formalism is also possible to improve the energetic estimations, again, these predictions should be thoroughly tested against further experimental data [56, 62].

First principles calculation tools are also nowadays available to explore the energetics of multicomponent condensed phases. They can calculate the thermodynamic properties for alloy systems as well as phase diagrams using the Alloy Theoretic Automated Toolkit (ATAT) [63], but this software is better equipped to handle structurally simpler alloys not liquid at or below room temperature. It requires assumptions regarding the entropy of mixing contributions in solutions, which cannot be directly accessed via such simulations. Moreover, the required precision to accurately predict phase transition temperatures (such as solidus and liquidus) solely on DFT simulations is not yet achievable [63, 64].

The purpose of the present communication is to provide a detailed description of the newly developed liquid metal solution calorimetry technique and its application to determine enthalpies of dissolution/mixing for the well-known eutectics of the binary Ga–In, the ternary Ga–In–Sn, and the quaternary Ga–In–Sn–Zn alloy systems [65]. The experimental enthalpy data are compared to energetic analogs calculated by different computational techniques. The general application of FactSage and the most common geometric models in comparison with the experimental data is also highlighted.

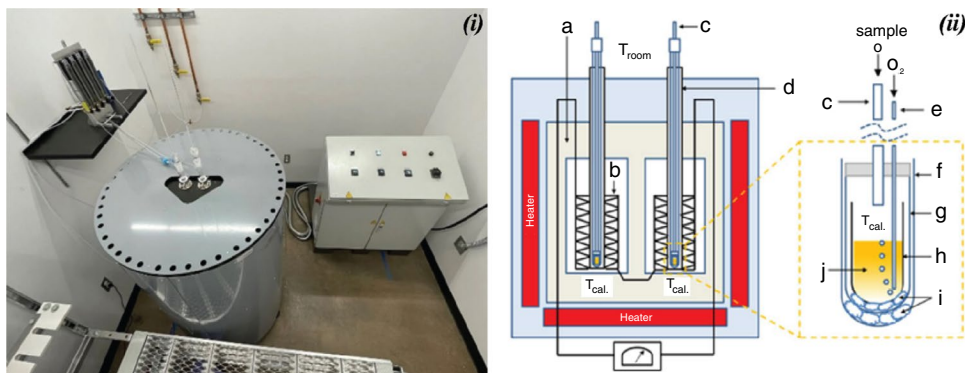
## Experimental methods

### Liquid metal solution calorimetry

The calorimetric experiments were carried out in a Tian-Calvet twin calorimeter (AlexSYS, Setaram, Caluire, France) at 800 °C, illustrated in Fig. 1.

For the glassware arrangement, instead of the standard off-center dropping and bubbling tube holes and smaller dropping tube radius, a new design with centered dropping and bubbling tube holes and a bigger radius (0.35" = 0.89 cm OD) was utilized and is pictured in Fig. 2(i)(b). This was done to minimize sample losses and contact with the glassware before reaching the solvent. These tubes, however, were not completely effective at minimizing the continued loss of liquid samples upon contact with the dropping tube. So, sodium molybdate solvent ( $3\text{Na}_2\text{O}\cdot 4\text{MoO}_3$ ) was explored to maintain consistent sample compositions and reduce the probabilities of liquid drop mass deviations by eliminating sample wobbling down the tube, allowing travel straight down to the calorimeter reaction chamber. A combination of sodium molybdate pieces ( $\geq 1$  mg,  $1/8'' = 0.32$  cm in length), 1:3 ratio of molybdenum oxide ( $\text{MoO}_3$ ) to sodium molybdate ( $\text{Na}_2\text{MoO}_4$ ), were coated in the center with liquid metal droplets (0.3–0.5 mg). Figure 2ii illustrates the sample dimensions and the Ga-LMA placement on these vessel-like pieces. Sodium molybdate pieces were used as the transport medium for these experiments because of their room temperature solid state, their ease of dissolution into the experimental solvent, no change in solvent composition after continuous drop experiments, and their well characterized and consistent heat effects [44]. To maintain a stable reaction environment within the calorimeter,  $\text{O}_2$  gas was flushed over ( $\sim 40$  mL  $\text{min}^{-1}$ ) and bubbled through ( $\sim 17$  mL  $\text{min}^{-1}$ ) the solvent. Bubbling was done using silica glass tubes instead of the typical platinum-tipped tubes to prevent any alloying reactions of the tube tips with the Ga-LMA at high temperatures [66].

**Fig. 1** **i** A photo of the AlexSYS calorimeter. **ii** An assembly scheme of the AlexSYS calorimeter: (a) Inconel block, (b) thermopile, (c) dropping tube, (d) protection tube, (e) bubbling tube, (f) silica liner, (g) silica inner crucible, (h) silica outer crucible, (i) silica wool, and (j) molten salt solvent (20 g per crucible) [39]



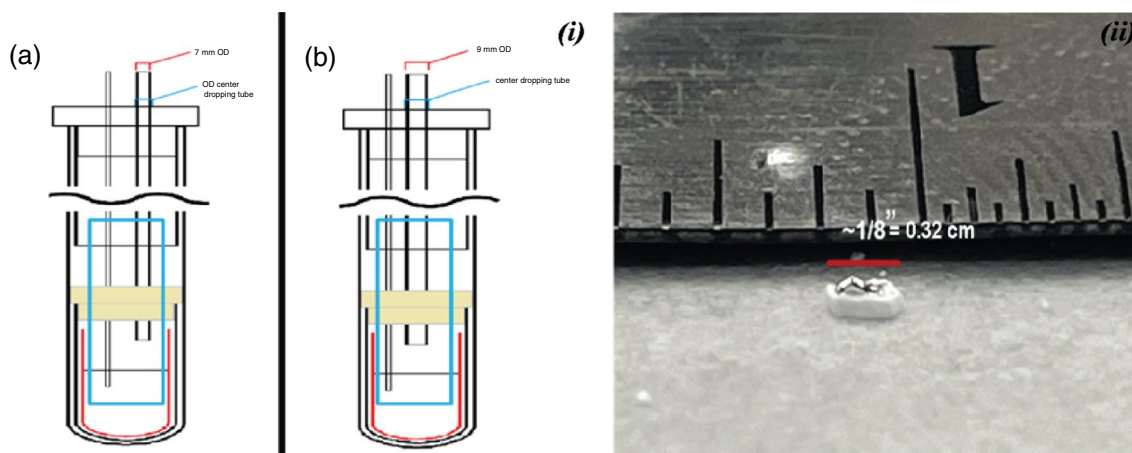


**Fig. 2** i (a) Original off-centered dropping tube (0.28" = 0.711 cm OD) (b) new centered dropping tube (0.35" = 0.89 cm OD). ii Prepped liquid metal sample with its respective sodium molybdate

vessel-like pellet for sample transport to calorimeter reaction chamber. For scale in inches a ruler is provided

The calorimeter calibration was done by dropping 3–4 mg of pressed benzoic acid pellets (Sigma Aldrich,  $\geq 99.5\%$ ). This calibrant best matches the experimental reaction conditions, where the majority of the heat effect comes from oxidation within the calorimeter rather than from heating the sample when dropped [67]. The calibration factors were calculated from the known enthalpy of combustion of benzoic acid and the heat contents of  $\text{CO}_2$  and  $\text{H}_2\text{O}$ . This calibration procedure is standard in our thermochemistry laboratory and has been described previously [35].

## Materials and characterization

For these experiments the initial constituent metals and the  $\text{Ga}_{0.835}\text{In}_{0.165}$  (GaIn) alloy were purchased from Sigma Aldrich and had a purity of 99.999% metal basis. The GaIn eutectic was used without further treatment.  $\text{Ga}_{0.782}\text{In}_{0.148}\text{Sn}_{0.070}$  (GaInSn) and  $\text{Ga}_{0.784}\text{In}_{0.147}\text{Sn}_{0.068}\text{Zn}_{0.011}$  (GaInSnZn) were synthesized with semi-spherical Ga/In specimens with diameters between 2 and 5 mm and the Sn/Zn samples were cut from 0.5 mm wires. The alloy samples were synthesized by melting the pure component metals in a sealed silica ampoule at 430 °C for 1 h. The risk of contamination by the oxygen was deemed insignificant. Since, synthesis was performed under vacuum after multiple purge cycles under Ar and under relatively low temperatures.

A semiquantitative analysis to measure homogeneity of the synthesized alloys was performed using a Helios 5 UX focused ion beam microscope (SEM-FIB) with energy dispersive analysis (EDX), operating at 15 kV and 1 nm resolution with accelerating electron voltages between 0.2 and 30 kV. The analyzed compositions for each of these were in reasonable agreement with the elemental mass fractions per gram of sample synthesized (see Table 1).

**Table 1** Elemental mass fractions per gram of sample synthesized and mole fractions ( $X_i$ ) determined with energy dispersive analysis (EDX) of GaInSn and GaInSnZn eutectics using a Helios 5 UX focused ion beam microscope (SEM-FIB) for semiquantitative composition determinations

Metals	Mases for GaInSn/g	$X_i$	Mases for GaInSnZn/g	$X_i$
Ga	0.68	0.79	0.69	0.82
In	0.21	0.13	0.21	0.11
Sn	0.10	0.083	0.10	0.067
Zn	N/A	N/A	0.0089	0.011

These compositions were not used in subsequent thermodynamic cycles. These data are only provided to prove sample homogeneity and compositional estimations

Finally, to make the vessel-like pieces of sodium molybdate, 20–30 mg of the standard solvent (1:3 ratio of  $\text{MoO}_3$  to  $\text{Na}_2\text{MoO}_4$ ) were melted at 700 °C for 5 min. These small amounts were melted to produce a thin solid disk with minimal thickness that was then broken to produce the small vessel-like pieces used in the experiments.

## Results and discussion

### Measured enthalpies of mixing

The enthalpies of oxidative drop solution and mixing from the metals are presented in Table 2. The average enthalpies of mixing of the liquid phase for each Ga-LMA can be determined from the drop solution enthalpies of their constituent metals corrected for the liquid state. For reference, all drop solution enthalpies reported previously along with the



**Table 2** Average enthalpies of drop solution ( $\Delta H_{ds}$ ) obtained for the room temperature liquid metal alloys dropped into sodium molybdate ( $3\text{Na}_2\text{O}\cdot 4\text{MoO}_3$ ) at 800 °C, the experimental enthalpies of mixing for

the multicomponent alloys at 25 °C, and the literature value found in Rugg et al. [24] for comparison

Composition	$\Delta H_{ds}/\text{kJ mol}^{-1}$	$\Delta_{\text{mix}}H/\text{kJ mol}^{-1}$	
		Experimental	Literature
GaIn ( $\text{Ga}_{0.835}\text{In}_{0.165}$ )	$-503.72 \pm 0.32$ (5)	$0.75 \pm 2.73$	$0.76 \pm 0.19$ [24]
GaInSn ( $\text{Ga}_{0.782}\text{In}_{0.148}\text{Sn}_{0.070}$ )	$-508.28 \pm 0.18$ (8)	$0.75 \pm 5.62$	
GaInSnZn ( $\text{Ga}_{0.784}\text{In}_{0.147}\text{Sn}_{0.068}\text{Zn}_{0.011}$ )	$-509.92 \pm 0.07$ (8)	$0.80 \pm 5.91$	

Experimental uncertainties are two standard deviations of the mean value and the numbers in parentheses are the number of samples dropped in this study. Alloy compositions were determined using values calculated from mass measurements to obtain highest compositional accuracy possible

**Table 3** Enthalpies of drop solution obtained by drop solution calorimetry ( $\Delta H_{ds}$ ) and enthalpies of fusion ( $\Delta H_{fus}$ ) for each of the constituent metals determined from melt enthalpies and heat content values in the literature, since Kopp’s law applies for the tested high order systems

Metals	$\Delta H_{ds}/\text{kJ mol}^{-1}$	$\Delta H_{fus}/\text{kJ mol}^{-1}$
Ga	$-501.40 \pm 1.44$ (9) [39]	5.70 [69]
In	$-475.00 \pm 1.93$ (8) [39]	7.10 [69]
Sn	$-553.07 \pm 5.08$ (8) [39]	13.00 [69]
Zn	$-342.460 \pm 1.85$ (8) [68]	18.10 [69]

Experimental uncertainties are two standard deviations of the mean value and the numbers in parentheses are the number of samples dropped and recorded in the literature provided

enthalpies of fusion for all constituent metals are provided in Table 3. These fusion values were calculated with literature melt enthalpies and heat content data, which effectively assume Kopp’s law applies for the tested high order eutectics [39, 68, 69]. The experimental enthalpies of mixing for the multicomponent liquid alloys at 25 °C were determined using the thermodynamic cycles found in Table 4.

For the GaIn eutectic, the experimental enthalpy of mixing shows excellent agreement with the literature value ( $0.75 \pm 2.73$  vs  $0.76 \pm 0.19$   $\text{kJ mol}^{-1}$  in Rugg et al.[24]), confirming the reliability and accuracy of liquid metal solution calorimetry. As mentioned above, there are no reported experimental values for the heat of mixing for the eutectics

**Table 4** Thermodynamic cycle for the enthalpies of mixing for GaIn, GaInSn, and GaInSnZn eutectics from the drop solution of the metals

$\text{Ga}_{0.835}\text{In}_{0.165}$ (l, 25 °C) + 0.750 $\text{O}_2$ (g, 800 °C) $\rightarrow$ 0.825 $\text{Ga}_2\text{O}_3$ (soln, 800 °C) + 0.418 $\text{In}_2\text{O}_3$ (soln, 800 °C)	$\Delta H_{ds \text{ GaIn(l)}}$
Ga (l, 25 °C) + 0.750 $\text{O}_2$ (g, 800 °C) $\rightarrow$ 0.500 $\text{Ga}_2\text{O}_3$ (soln, 800 °C)	$\Delta H_{ds \text{ Ga(l)}} = \Delta H_{ds \text{ Ga(s)}} - \Delta H_{fus \text{ Ga}}$
In (l, 25 °C) + 0.750 $\text{O}_2$ (g, 800 °C) $\rightarrow$ 0.500 $\text{In}_2\text{O}_3$ (soln, 800 °C)	$\Delta H_{ds \text{ In(l)}} = \Delta H_{ds \text{ In(s)}} - \Delta H_{fus \text{ In}}$
$0.835 \text{ Ga (l, 25 °C)} + 0.165 \text{ In (l, 25 °C)} \rightarrow \text{Ga}_{0.835}\text{In}_{0.165}$ (l, 25 °C)	
$\Delta_{\text{Mix}}H = -\Delta H_{ds \text{ GaIn(l)}} + (0.835 \Delta H_{ds \text{ Ga(l)}} + 0.165 \Delta H_{ds \text{ In(l)}})$	
$\text{Ga}_{0.782}\text{In}_{0.148}\text{Sn}_{0.070}$ (l, 25 °C) + 0.768 $\text{O}_2$ (g, 800 °C) $\rightarrow$ 0.391 $\text{Ga}_2\text{O}_3$ (soln, 800 °C) + 0.074 $\text{In}_2\text{O}_3$ (soln, 800 °C) + 0.070 $\text{SnO}_2$ (soln, 800 °C)	$\Delta H_{ds \text{ GaInSn(l)}}$
Ga (l, 25 °C) + 0.750 $\text{O}_2$ (g, 800 °C) $\rightarrow$ 0.500 $\text{Ga}_2\text{O}_3$ (soln, 800 °C)	$\Delta H_{ds \text{ Ga(l)}} = \Delta H_{ds \text{ Ga(s)}} - \Delta H_{fus \text{ Ga}}$
$0.835 \text{ In (l, 25 °C)} + 0.750 \text{ O}_2 \text{ (g, 800 °C)} \rightarrow 0.500 \text{ In}_2\text{O}_3 \text{ (soln, 800 °C)}$	$\Delta H_{ds \text{ In(l)}} = \Delta H_{ds \text{ In(s)}} - \Delta H_{fus \text{ In}}$
$\text{Sn (l, 25 °C)} + \text{O}_2 \text{ (g, 800 °C)} \rightarrow \text{SnO}_2 \text{ (soln, 800 °C)}$	$\Delta H_{ds \text{ Sn(l)}} = \Delta H_{ds \text{ Sn(s)}} - \Delta H_{fus \text{ Sn}}$
$0.782 \text{ Ga (l, 25 °C)} + 0.148 \text{ In (l, 25 °C)} + 0.070 \text{ Sn (l, 25 °C)} \rightarrow \text{Ga}_{0.782}\text{In}_{0.148}\text{Sn}_{0.070}$ (l, 25 °C)	
$\Delta_{\text{Mix}}H = -\Delta H_{ds \text{ GaInSn(l)}} + (0.782 \Delta H_{ds \text{ Ga(l)}} + 0.148 \Delta H_{ds \text{ In(l)}} + 0.070 \Delta H_{ds \text{ Sn(l)}})$	
$\text{Ga}_{0.784}\text{In}_{0.147}\text{Sn}_{0.068}\text{Zn}_{0.011}$ (l, 25 °C) + 1.764 $\text{O}_2$ (g, 800 °C) $\rightarrow$ 0.392 $\text{Ga}_2\text{O}_3$ (soln, 800 °C) + 0.074 $\text{In}_2\text{O}_3$ (soln, 800 °C) + 0.068 $\text{SnO}_2$ (soln, 800 °C) + 0.011 $\text{ZnO}$ (soln, 800 °C) + 0.070 $\text{SnO}_2$ (soln, 800 °C)	$\Delta H_{ds \text{ GaInSnZn(l)}}$
Ga (l, 25 °C) + 0.750 $\text{O}_2$ (g, 800 °C) $\rightarrow$ 0.500 $\text{Ga}_2\text{O}_3$ (soln, 800 °C)	$\Delta H_{ds \text{ Ga(l)}} = \Delta H_{ds \text{ Ga(s)}} - \Delta H_{fus \text{ Ga}}$
In (l, 25 °C) + 0.750 $\text{O}_2$ (g, 800 °C) $\rightarrow$ 0.500 $\text{In}_2\text{O}_3$ (soln, 800 °C)	$\Delta H_{ds \text{ In(l)}} = \Delta H_{ds \text{ In(s)}} - \Delta H_{fus \text{ In}}$
$\text{Sn (l, 25 °C)} + \text{O}_2 \text{ (g, 800 °C)} \rightarrow \text{SnO}_2 \text{ (soln, 800 °C)}$	$\Delta H_{ds \text{ Sn(l)}} = \Delta H_{ds \text{ Sn(s)}} - \Delta H_{fus \text{ Sn}}$
$\text{Zn (l, 25 °C)} + 0.500 \text{ O}_2 \text{ (g, 800 °C)} \rightarrow \text{ZnO (soln, 800 °C)}$	$\Delta H_{ds \text{ Zn(l)}} = \Delta H_{ds \text{ Zn(s)}} - \Delta H_{fus \text{ Zn}}$
$0.784 \text{ Ga (l, 25 °C)} + 0.147 \text{ In (l, 25 °C)} + 0.068 \text{ Sn (l, 25 °C)} + 0.011 \text{ Zn (l, 25 °C)} \rightarrow \text{Ga}_{0.784}\text{In}_{0.147}\text{Sn}_{0.068}\text{Zn}_{0.011}$ (l, 25 °C)	
$\Delta_{\text{Mix}}H = -\Delta H_{ds \text{ GaInSnZn(l)}} + (0.784 \Delta H_{ds \text{ Ga(l)}} + 0.147 \Delta H_{ds \text{ In(l)}} + 0.068 \Delta H_{ds \text{ Sn(l)}} + 0.011 \Delta H_{ds \text{ Zn(l)}})$	

Ga, In, Sn, and Zn are the metals in question, s, g, l, soln mean solid phase, gas phase, liquid phase, and solution in molten sodium molybdate respectively. The enthalpies of drop solution calorimetry, fusion, and mixing are denoted by  $\Delta H_{ds}$ ,  $\Delta H_{fus}$ , and  $\Delta H_{\text{Mix}}$  respectively

of the ternary Ga–In–Sn or the quaternary Ga–In–Sn–Zn systems, so multiple computational methods were employed for comparisons to the experimental data (Fig. 3).

### Geometrical models and FactSage software computations

To compare the experimental heats of mixing for the ternary and quaternary eutectics, both symmetric and asymmetric

models were computed along with the FactSage software (using the FTlite database), these are given in Table 5 and Fig. 4, showing agreement within the obtained experimental uncertainty for the ternary and quaternary alloys. The values closest to the experimental data were those obtained by the Hillert and Chou models [50, 54]. Based on a root mean square analysis (RMSD) performed on all the computational methods for eutectics of Ga–In–Sn and Ga–In–Sn–Zn alloys (see Table 2). The formulation used for this analysis was

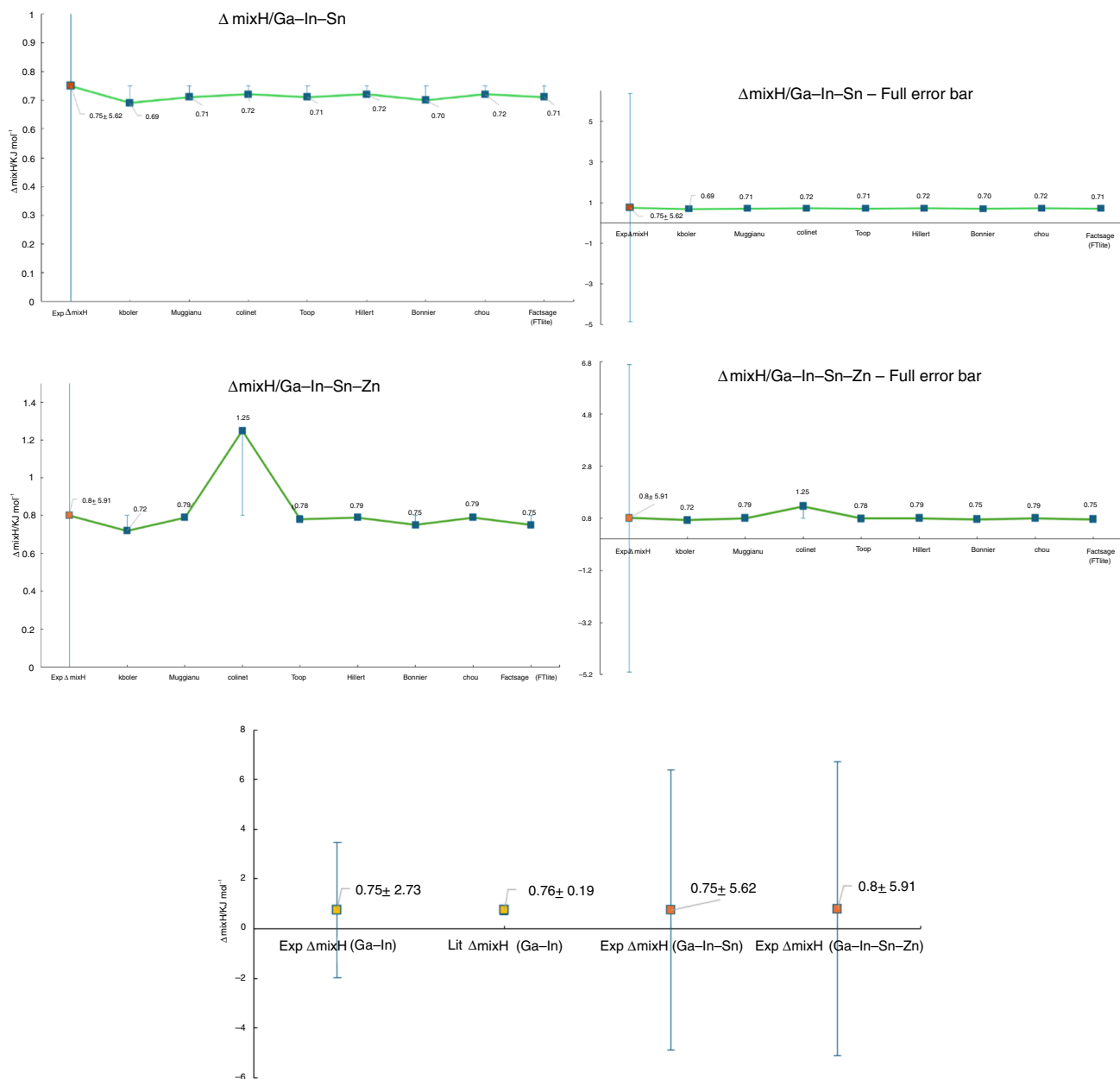


**Fig. 3** Experimental heats of mixing (orange squares) for the eutectics of the Ga–In–Sn (top two) and Ga–In–Sn–Zn systems (middle two) compared to modeling results (blue squares) for all calculation methods employed. Tabulated experimental heat of mixing in this

study and literature value (bottom center) for the eutectics of the Ga–In (yellow squares), Ga–In–Sn, and Ga–In–Sn–Zn systems (orange squares). (Color figure online)

**Table 5** All mixing enthalpies produced by the geometrical models and FactSage for GaInSn and GaInSnZn eutectics used for comparison with the obtained experimental data by the calculation of the mean square deviation value (RMSD)

Models	$\Delta_{\text{mix}}H/\text{kJ mol}^{-1}$ (GaInSn)	$\Delta_{\text{mix}}H/\text{kJ mol}^{-1}$ (GaInSnZn)	RMSD (GaInSn)	RMSD (GaInSnZn)
Kohler	0.69	0.72	0.06	0.08
Maggianu	0.71	0.79	0.04	0.01
Colinet	0.72	1.25	0.03	0.45
Toop	0.71	0.78	0.04	0.02
Hillert	0.72	0.79	0.03	0.01
Bonnier	0.70	0.75	0.05	0.05
Chou	0.72	0.79	0.03	0.01
FactSage- FTlite	0.71	0.75	0.04	0.05

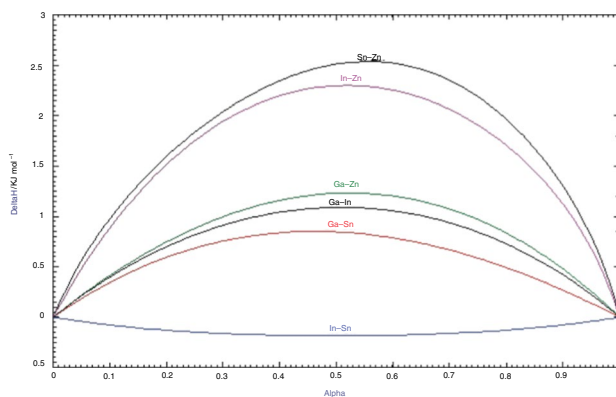


**Fig. 4** Enthalpy of mixing (reference state: pure liquids at 25 °C) of the binary liquid subsystems as calculated using the FTlite database of the FactSage 8.2 software. Used to determine the enthalpies of mixing in the models discussed above. *Note* only the liquid solution was considered for these calculations. Alpha stands for the molar composition range between A and B

summarized and can be found in the literature [70]. The RMSD values for Hillert model were 0.03 for GaInSn and 0.01 GaInSnZn. The Chou model, similarly, gave 0.03 for GaInSn and 0.01 GaInSnZn. These values represent the minimal magnitude of the difference between experimental and computed energetics for both GaInSn and GaInSnZn, supporting compositional asymmetry in the heats of mixing, especially for the quaternary eutectic, but complete calorimetric studies are needed to confirm the detailed behavior. FactSage appears to be the most effective calculation method because it handles the thermodynamics of liquid multicomponent alloys quickly and effectively with reasonable accuracy [56]. This software also offers tunability to produce more accurate results while providing an extensively optimized database of binary alloys to compute the mixing

enthalpies of higher order solutions. For the geometrical models described above, the calculations were accomplished by inputting the binary enthalpy outputs from the Flite database (see Fig. 4) into each model and computing the energetics through EXCEL.

The small differences between the calculated energies by FactSage and the experimental values, though within experimental uncertainty, may suggest energetic effects not explicitly accounted for by the current CALPHAD-based computational formalisms used in thermodynamic packages [56]. The necessity to account for the strength of each individual two-body interaction (via classical interatomic potentials which also depend on interatomic distances) as well as for the internal structure of the studied melts may provide more accurate predictions than the optimization of the interpolation method (i.e. symmetric vs asymmetric) [71].

Possible benefits of using the newly developed liquid metal solution calorimetry technique for future work include extending its application to more Ga-LMA and other potential liquid at or below room temperature materials [72]. Now that the values of the enthalpy of drop solution for the eutectics of the Ga–In and Ga–In–Sn alloys are determined, future study of more complex Ga-LMA require only the measurements of the heat of drop solution of the multicomponent samples, greatly decreasing the work needed to analyze their heats of formation and mixing. This calculation process, as detailed in other research [35], can be applied to Ga alloys consisting of many more constituents, not just up to the quaternary systems. Another advantage of this technique is the reproducible final states and low concentrations of the dissolved products, making the heats of solution obtained independent from the concentration of dissolved species present in the solvent, the interactions of the cations in the melt, or precipitation of inter oxidic compounds during experiments [43]. As all other solution calorimetric techniques, this method requires complete and reasonably rapid reactions and dissolution of samples that must be verified for any new system to be studied. It is likely that some Ga-LMA alloy systems will not easily meet these requirements and further modifications of this technique may be necessary. [35, 65].

## Conclusions

Oxidative solution calorimetry was refined to measure the mixing enthalpies of Ga-LMA and verified with the characterization of the Ga–In, Ga–In–Sn, and Ga–In–Sn–Zn eutectic compositions. This involved redesigning the calorimetric glassware and the creation of a transport system to enable reliable dropping of molten metal samples from room temperature into molten sodium molybdate solvent at 800 °C in a Calvet microcalorimeter. This technique will enable future work in more complex higher order Ga-LMA as well

as other material systems liquid at or below ambient temperature, advancing both the experimental thermodynamics and metallurgy fields. Analyses employing the geometric mixing models (symmetric/asymmetric) and FactSage showed agreement within experimental uncertainty, favoring asymmetric mixing properties, especially for the GaInSnZn eutectic. All these empirical methods suggest appropriate enthalpy analogs for unknown and increasingly complex alloy systems to be analyzed through high temperature oxidative solution calorimetry in the future.

**Supplementary Information** The online version contains supplementary material available at <https://doi.org/10.1007/s10973-024-13035-5>.

**Acknowledgements** This work was supported by the U.S. Department of Energy, Office of Basic Energy Sciences, Materials Science, and Engineering Division, grant DE-SC0021987. We acknowledge the use of facilities within the Eyring Materials Center at Arizona State University.

**Author contributions** M. Bustamante: Conceptualization, methodology development, performance of all experiments, writing of original draft, review, and editing. K. Lilova: Conceptualization, assistance with experiments, writing of original draft, review, and editing. A. Navrotsky: Conceptualization, writing of the original draft, review, and editing. J.-P. Harvey: FactSage calculations, review, and editing. O. Kentaro: FactSage calculations and review.

## Declarations

**Conflict of interest** The authors declare that they have no known competing financial interests or personal relationships that could have appeared to influence the work reported in this article.

## References

- Wang X, Guo R, Liu J. Liquid metal based soft robotics materials, designs, and applications. *Adv Mater Technol*. 2018. <https://doi.org/10.1002/admt.201800549>.
- Liu S, Sweatman K, McDonald S, Nogita K. Ga-based alloys in microelectronic interconnects: a review. *Mater Basel Switz*. 2018;11(8):1384. <https://doi.org/10.3390/ma11081384>.
- Kidanu WG, Hur J, Kim IT. Gallium-Indium-Tin eutectic as a self-healing room-temperature liquid metal anode for high-capacity lithium-ion batteries. *Mater Basel Switz*. 2021;15(1):168. <https://doi.org/10.3390/ma15010168>.
- Aukarasereenont P, Goff A, Nguyen CK, McConville CF, Elbourne A, Zavabeti A, Daeneke T. Liquid metals: an ideal platform for the synthesis of two-dimensional materials. *Chem Soc Rev*. 2022;51(4):1253–76. <https://doi.org/10.1039/D1CS01166A>.
- Narh KA, Dwivedi VP, Grow JM, Stana A, Shih W-Y. The effect of liquid gallium on the strengths of stainless steel and thermoplastics. *J Mater Sci*. 1998;33(2):329–37. <https://doi.org/10.1023/A:1004359410957>.
- Ren L, Xu X, Du Y, Kalantar-Zadeh K, Dou SX. Liquid metals and their hybrids as stimulus-responsive smart materials. *Mater Today*. 2020;34:92–114. <https://doi.org/10.1016/j.mattod.2019.10.007>.
- Ma K-Q, Liu J. Nano liquid-metal fluid as ultimate coolant. *Phys Lett A*. 2007;361(3):252–6. <https://doi.org/10.1016/j.physleta.2006.09.041>.
- Wang H, Peng Y, Peng H, Zhang J. Fluidic phase-change materials with continuous latent heat from theoretically tunable ternary metals for efficient thermal management. *Proc Natl Acad Sci U S A*. 2022;119(31): e2200223119. <https://doi.org/10.1073/pnas.2200223119>.
- Shamberger PJ, Bruno NM. Review of metallic phase change materials for high heat flux transient thermal management applications. *Appl Energy*. 2020;258: 113955. <https://doi.org/10.1016/j.apenergy.2019.113955>.
- Deng Y-G, Liu J. Corrosion development between liquid gallium and four typical metal substrates used in chip cooling device. *Appl Phys A*. 2009;95(3):907–15. <https://doi.org/10.1007/s00339-009-5098-1>.
- Tang S-Y, Tabor C, Kalantar-Zadeh K, Dickey MD. Gallium liquid metal: the devil's elixir. *Annu Rev Mater Res*. 2021;51(1):381–408. <https://doi.org/10.1146/annurev-matsci-080819-125403>.
- Liu S, Li P, Zeng D. Research progress of liquid metal induced corrosion. *Corros Sci Prot Technology*. 2001;13(5):275–8.
- Daalkhajav U, Yirmibesoglu OD, Walker S, Mengüç Y. Rheological modification of liquid metal for additive manufacturing of stretchable electronics. *Adv Mater Technol*. 2018;3(4):1700351. <https://doi.org/10.1002/admt.201700351>.
- Kong W, Wang Z, Wang M, Manning KC, Uppal A, Green MD, Wang RY, Rykaczewski K. Oxide-mediated formation of chemically stable tungsten-liquid metal mixtures for enhanced thermal interfaces. *Adv Mater*. 2019;31(44):1904309. <https://doi.org/10.1002/adma.201904309>.
- Kong W, Wang Z, Casey N, Korah MM, Uppal A, Green MD, Rykaczewski K, Wang RY. High thermal conductivity in multiphase liquid metal and silicon carbide soft composites. *Adv Mater Interfaces*. 2021;8(14):2100069. <https://doi.org/10.1002/admi.202100069>.
- Idrus-Saidi SA, Tang J, Lambie S, Han J, Mayyas M, Ghasemian MB, Allieux F-M, Cai S, Koshy P, Mostaghimi P, Steenbergen KG, Barnard AS, Daeneke T, Gaston N, Kalantar-Zadeh K. Liquid metal synthesis solvents for metallic crystals. *Science*. 2022;378(6624):1118–24. <https://doi.org/10.1126/science.abm2731>.
- Degtyareva O, McMahon MI, Allan DR, Nelmes RJ. Structural complexity in gallium under high pressure: relation to alkali elements. *Phys Rev Lett*. 2004;93(20): 205502. <https://doi.org/10.1103/PhysRevLett.93.205502>.
- Yu Q, Ahmad AS, Ståhl K, Wang XD, Su Y, Glazyrin K, Liermann HP, Franz H, Cao QP, Zhang DX, Jiang JZ. Pressure-induced structural change in liquid gain eutectic alloy. *Sci Rep*. 2017;7(1):1139. <https://doi.org/10.1038/s41598-017-01233-1>.
- Koh A, HwangZavalij WYP, Chun S, Slipher G, Mrozek R. Solidification and melting phase change behavior of eutectic Gallium-Indium-Tin. *Materialia*. 2019;8:100512. <https://doi.org/10.1016/j.mtla.2019.100512>.
- Zabrocki M, Gaşior W, Dębski A. Thermodynamic properties of Ga-In-Li alloys—a potential material for liquid metal batteries. *J Mol Liq*. 2021;332: 115765. <https://doi.org/10.1016/j.molliq.2021.115765>.
- Jendrzejczyk-Handzlik D, Handzlik P. Enthalpies of mixing of liquid Ga-In and Cu-Ga-In alloys. *J Mol Liq*. 2019;293: 111543. <https://doi.org/10.1016/j.molliq.2019.111543>.
- Perona-Silhol N, Gambino M, Bros JP, Hoch M. The Cd-Ga-In-Sn-Zn liquid system. Experimental and predicted values of the enthalpy of formation. *J Alloy Compd*. 1992;189(1):17–22. [https://doi.org/10.1016/0925-8388\(92\)90040-G](https://doi.org/10.1016/0925-8388(92)90040-G).
- Ansara I, Gambino M, Bros JP. Étude thermodynamique du système ternaire gallium-indium-antimoine. *J Cryst Growth*. 1976;32(1):101–10. [https://doi.org/10.1016/0022-0248\(76\)90016-6](https://doi.org/10.1016/0022-0248(76)90016-6).



24. Rugg BC, Chart TG. A critical assessment of thermodynamic and phase diagram data for the gallium-indium system. *Calphad*. 1990;14(2):115–23. [https://doi.org/10.1016/0364-5916\(90\)90013-P](https://doi.org/10.1016/0364-5916(90)90013-P).
25. Kulawik S, Gierlotka W, Dębski A, Gašior W, Zajączkowski A. Calorimetric and phase diagram studies of the Ga–In–Zn system. *J Mol Liq*. 2021;325: 115114. <https://doi.org/10.1016/j.molliq.2020.115114>.
26. Gomidželović L, Živković D, Kostov A, Mitovski A, Balanović L. Comparative thermodynamic study of Ga–In–Sb system. *J Therm Anal Calorim*. 2011;103(3):1105–9. <https://doi.org/10.1007/s10973-010-1203-0>.
27. Meschel SV, Kleppa OJ. The standard enthalpies of formation of some intermetallic compounds of transition metals by high temperature direct synthesis calorimetry. *J Alloy Compd*. 2006;415(1–2):143–9. <https://doi.org/10.1016/j.jallcom.2005.08.006>.
28. Meschel SV, Kleppa OJ. Thermochemistry of some binary alloys of samarium with the noble metals (Cu, Ag, Au) by high temperature direct synthesis calorimetry. *J Alloy Compd*. 2006;416(1–2):93–7. <https://doi.org/10.1016/j.jallcom.2005.07.069>.
29. Ferro R, Borzone G, Cacciamani G, Parodi N. Thermodynamics of rare earth alloys: systematics and experimental. *Thermochim Acta*. 1998;314(1–2):183–204. [https://doi.org/10.1016/S0040-6031\(98\)00266-4](https://doi.org/10.1016/S0040-6031(98)00266-4).
30. Meschel SV, Kleppa OJ. Thermochemistry of alloys of transition metals and lanthanide metals with some IIIB and IVB elements in the periodic table. *J Alloy Compd*. 2001;321(2):183–200. [https://doi.org/10.1016/S0925-8388\(01\)00966-5](https://doi.org/10.1016/S0925-8388(01)00966-5).
31. Guo Q, Kleppa OJ. The standard enthalpies of formation of the compounds of early transition metals with late transition metals and with noble metals as determined by Kleppa and co-workers at the University of Chicago—a review. *J Alloy Compd*. 2001;321(2):169–82. [https://doi.org/10.1016/S0925-8388\(01\)00956-2](https://doi.org/10.1016/S0925-8388(01)00956-2).
32. Colinet C. High temperature calorimetry: recent developments. *J Alloy Compd*. 1995;220(1–2):76–87. [https://doi.org/10.1016/0925-8388\(94\)06032-0](https://doi.org/10.1016/0925-8388(94)06032-0).
33. Selhaoui N, Gachon J-C, Hertz J. Enthalpies of formation of some solid hafnium nickel compounds and of the Ni-rich HfNi liquid by direct reaction calorimetry. *Metall Trans B*. 1992;23(6):815–9. <https://doi.org/10.1007/BF02656460>.
34. Borzone G, Borsese A, Ferro R. A contribution to the study of the alloying behaviour of the rare earths with tin. *Z Für Anorg Allg Chem*. 1983;501(6):199–208. <https://doi.org/10.1002/zaac.19835010624>.
35. Hayun S, Lilova K, Salhov S, Navrotsky A. Enthalpies of formation of high entropy and multicomponent alloys using oxide melt solution calorimetry. *Intermetallics*. 2020;125: 106897. <https://doi.org/10.1016/j.intermet.2020.106897>.
36. Kleppa OJ. A new high temperature reaction calorimeter: the heats of mixing of liquid lead-tin alloys. *J Phys Chem*. 1955;59(2):175–81. <https://doi.org/10.1021/j150524a020>.
37. Bros JP. High-temperature calorimetry in metallurgy. *J Common Met*. 1989;154(1):9–30. [https://doi.org/10.1016/0022-5088\(89\)90166-5](https://doi.org/10.1016/0022-5088(89)90166-5).
38. Tmar M, Pasturel A, Colinet C. Thermodynamics of (Silicon + Indium) and (Silicon + Gallium) Calorimetric determination of the partial molar enthalpy at infinite dilution of Si in indium and gallium. *J Chem Thermodyn*. 1983;15(11):1037–40. [https://doi.org/10.1016/0021-9614\(83\)90029-0](https://doi.org/10.1016/0021-9614(83)90029-0).
39. Abramchuk M, Lilova K, Subramani T, Yoo R, Navrotsky A. Development of high-temperature oxide melt solution calorimetry for p-block element containing materials. *J Mater Res*. 2020;35(16):2239–46. <https://doi.org/10.1557/jmr.2020.185>.
40. Subramani T, Lilova K, Abramchuk M, Leinenweber KD, Navrotsky A. Greigite (Fe<sub>3</sub>S<sub>4</sub>) is thermodynamically stable: implications for its terrestrial and planetary occurrence. *Proc Natl Acad Sci*. 2020;117(46):28645–8. <https://doi.org/10.1073/pnas.2017312117>.
41. Majzlan J, Kiefer S, Lilova K, Subramani T, Navrotsky A, Tuhý M, Vymazalová A, Chareev DA, Dachs E, Benisek A. Calorimetric study of skutterudite (CoAs<sub>2</sub>92) and heazlewoodite (Ni<sub>3</sub>S<sub>2</sub>). *Am Miner*. 2022;107(12):2219–25. <https://doi.org/10.2138/am-2022-8337>.
42. Navrotsky A, Rapp RP, Smelik E, Burnley P, Circone S, Chai L, Bose K. The behavior of H<sub>2</sub>O and CO<sub>2</sub> in high-temperature lead borate solution calorimetry of volatile-bearing phases. *Am Miner*. 1994;79(11–12):1099–109.
43. Navrotsky A. Progress and new directions in calorimetry: a 2014 perspective. *J Am Ceram Soc*. 2014;97(11):3349–59. <https://doi.org/10.1111/jace.13278>.
44. Navrotsky A. Progress and new directions in high temperature calorimetry. *Phys Chem Miner*. 1977;2(1):89–104. <https://doi.org/10.1007/BF00307526>.
45. Navrotsky A. Progress and new directions in high temperature calorimetry revisited. *Phys Chem Miner*. 1997;24(3):222–41. <https://doi.org/10.1007/s002690050035>.
46. Deore S. Oxide melt solution calorimetry of sulfides: enthalpy of formation of sphalerite, galena, greenockite, and hawleyite. *Am Miner*. 2006;91(2–3):400–3. <https://doi.org/10.2138/am.2006.1921>.
47. Deore S, Xu F, Navrotsky A. Oxide-melt solution calorimetry of selenides: enthalpy of formation of zinc, cadmium, and lead selenide. *Am Miner*. 2008;93(5–6):779–83. <https://doi.org/10.2138/am.2008.2752>.
48. Brown E. Hematite-ilmenite (Fe<sub>2</sub>O<sub>3</sub>–FeTiO<sub>3</sub>) solid solutions: the effects of cation ordering on the thermodynamics of mixing. *Am Miner*. 1994;79(5–6):485–96.
49. Kattner UR. The Calphad method and its role in material and process development. *Tecnol Em Metal Mater E Min*. 2016;13(1):3–15. <https://doi.org/10.4322/2176-1523.1059>.
50. Hillert M. Empirical methods of predicting and representing thermodynamic properties of ternary solution phases. *Calphad*. 1980;4(1):1–12. [https://doi.org/10.1016/0364-5916\(80\)90016-4](https://doi.org/10.1016/0364-5916(80)90016-4).
51. Miedema AR. Simple model for alloys. 1973;33.
52. Li C, Yuan Y, Li F, Wei Q, Huang Y. Modification and verification of miedema model for predicating thermodynamic properties of binary precipitates in multi-element alloys. *Phys B Condens Matter*. 2022;627: 413540. <https://doi.org/10.1016/j.physb.2021.413540>.
53. Ouyang Y, Zhong X, Du Y, Jin Z, He Y, Yuan Z. Formation enthalpies of Fe–Al–RE ternary alloys calculated with a geometric model and Miedema’s theory. *J Alloys Compd*. 2006;416(1–2):148–54. <https://doi.org/10.1016/j.jallcom.2005.08.055>.
54. Chou K-C. A general solution model for predicting ternary thermodynamic properties. *Calphad*. 1995;19(3):315–25. [https://doi.org/10.1016/0364-5916\(95\)00029-E](https://doi.org/10.1016/0364-5916(95)00029-E).
55. Chou K-C, Li W-C, Li F, He M. Formalism of new ternary model expressed in terms of binary regular-solution type parameters. *Calphad*. 1996;20(4):395–406. [https://doi.org/10.1016/S0364-5916\(97\)00002-3](https://doi.org/10.1016/S0364-5916(97)00002-3).
56. Kattner UR. The need for reliable data in computational thermodynamics. *High Temp-High Press*. 2020;49:1–2.
57. Ouyang Y, Zhong X, Du Y, Feng Y, He Y. Enthalpies of formation for the Al–Cu–Ni–Zr quaternary alloys calculated via a combined approach of geometric model and Miedema theory. *J Alloys Compd*. 2006;420(1–2):175–81. <https://doi.org/10.1016/j.jallcom.2005.10.047>.
58. Bale CW, Chartrand P, Degterov SA, Eriksson G, Hack K, Ben Mahfoud R, Melançon J, Pelton AD, Petersen S.

- FactSage thermochemical software and databases. *Calphad*. 2002;26(2):189–228. [https://doi.org/10.1016/S0364-5916\(02\)00035-4](https://doi.org/10.1016/S0364-5916(02)00035-4).
59. Sundman B, Kattner UR, Palumbo M, Fries SG. OpenCalphad—a free thermodynamic software. *Integr Mater Manuf Innov*. 2015;4(1):1–15. <https://doi.org/10.1186/s40192-014-0029-1>.
60. Otis R, Liu Z-K. Pycalphad: CALPHAD-based computational thermodynamics in python. *J Open Res Softw*. 2017;5(1):1. <https://doi.org/10.5334/jors.140>.
61. Andersson J-O, Helander T, Höglund L, Shi P, Sundman B. Thermo-Calc & DICTRA, computational tools for materials science. *Calphad*. 2002;26(2):273–312. [https://doi.org/10.1016/S0364-5916\(02\)00037-8](https://doi.org/10.1016/S0364-5916(02)00037-8).
62. Harvey J-P, Lebreux-Desilets F, Marchand J, Oishi K, Bouarab A-F, Robelin C, Gheribi AE, Pelton AD. On the application of the FactSage thermochemical software and databases in materials science and pyrometallurgy. *Processes*. 2020;8(9):1156. <https://doi.org/10.3390/pr8091156>.
63. van de Walle A, Asta M, Ceder G. The alloy theoretic automated toolkit: a user guide. *Calphad*. 2002;26(4):539–53. [https://doi.org/10.1016/S0364-5916\(02\)80006-2](https://doi.org/10.1016/S0364-5916(02)80006-2).
64. Liu ZK, Chen LQ. Integration of first-principles calculations, Calphad modeling, and phase-field simulations. In: Bozzolo G, Noebe RD, Abel PB, Vij DR, editors. *Applied computational materials modeling*. US: Boston, MA: Springer; 2007. p 171–213. [https://doi.org/10.1007/978-0-387-34565-9\\_6](https://doi.org/10.1007/978-0-387-34565-9_6).
65. Yu D, Xue Z, Mu T. Eutectics: formation, properties, and applications. *Chem Soc Rev*. 2021;50(15):8596–638. <https://doi.org/10.1039/D1CS00404B>.
66. Okamoto H. Ga-Pt (Gallium-Platinum). *J Phase Equilibria Diffus*. 2007;28(5):494–494. <https://doi.org/10.1007/s11669-007-9149-z>.
67. Zivkovic D, Manasijevic D, Zivkovic Z. Thermodynamic study of Ga-Sn and Ga-Zn systems using quantitative differential thermal analysis. *J Therm Anal Calorim*. 2003;74(1):85–96. <https://doi.org/10.1023/A:1026373602352>.
68. Subramani T, Lilova K, Householder M, Yang S, Lyons J, Navrotsky A. Surface energetics of wurtzite and sphalerite polymorphs of zinc sulfide and implications for their formation in nature. *Geochim Cosmochim Acta*. 2023;340:99–107. <https://doi.org/10.1016/j.gca.2022.11.003>.
69. Barin I. Thermochemical data of pure substances. 1st ed. Wiley; 1995. <https://doi.org/10.1002/9783527619825>.
70. Maniani ME, Sabbar A. Partial and integral enthalpies of mixing in the liquid Ag–In–Sn–Zn quaternary alloys. *Thermochim Acta*. 2014;592:1–9. <https://doi.org/10.1016/j.tca.2014.07.028>.
71. Harvey J-P, Gheribi AE, Rincant A, Jofré J, Lafaye P. On the elaboration of the next generation of thermodynamic models of solid solutions. *Phys Chem Chem Phys*. 2020;22(35):19999–20013. <https://doi.org/10.1039/D0CP02642E>.
72. Bara JE, Camper DE, Gin DL, Noble RD. Room-temperature ionic liquids and composite materials: platform technologies for CO<sub>2</sub> capture. *Acc Chem Res*. 2010;43(1):152–9. <https://doi.org/10.1021/ar9001747>.

**Publisher's Note** Springer Nature remains neutral with regard to jurisdictional claims in published maps and institutional affiliations.

Springer Nature or its licensor (e.g. a society or other partner) holds exclusive rights to this article under a publishing agreement with the author(s) or other rightsholder(s); author self-archiving of the accepted manuscript version of this article is solely governed by the terms of such publishing agreement and applicable law.